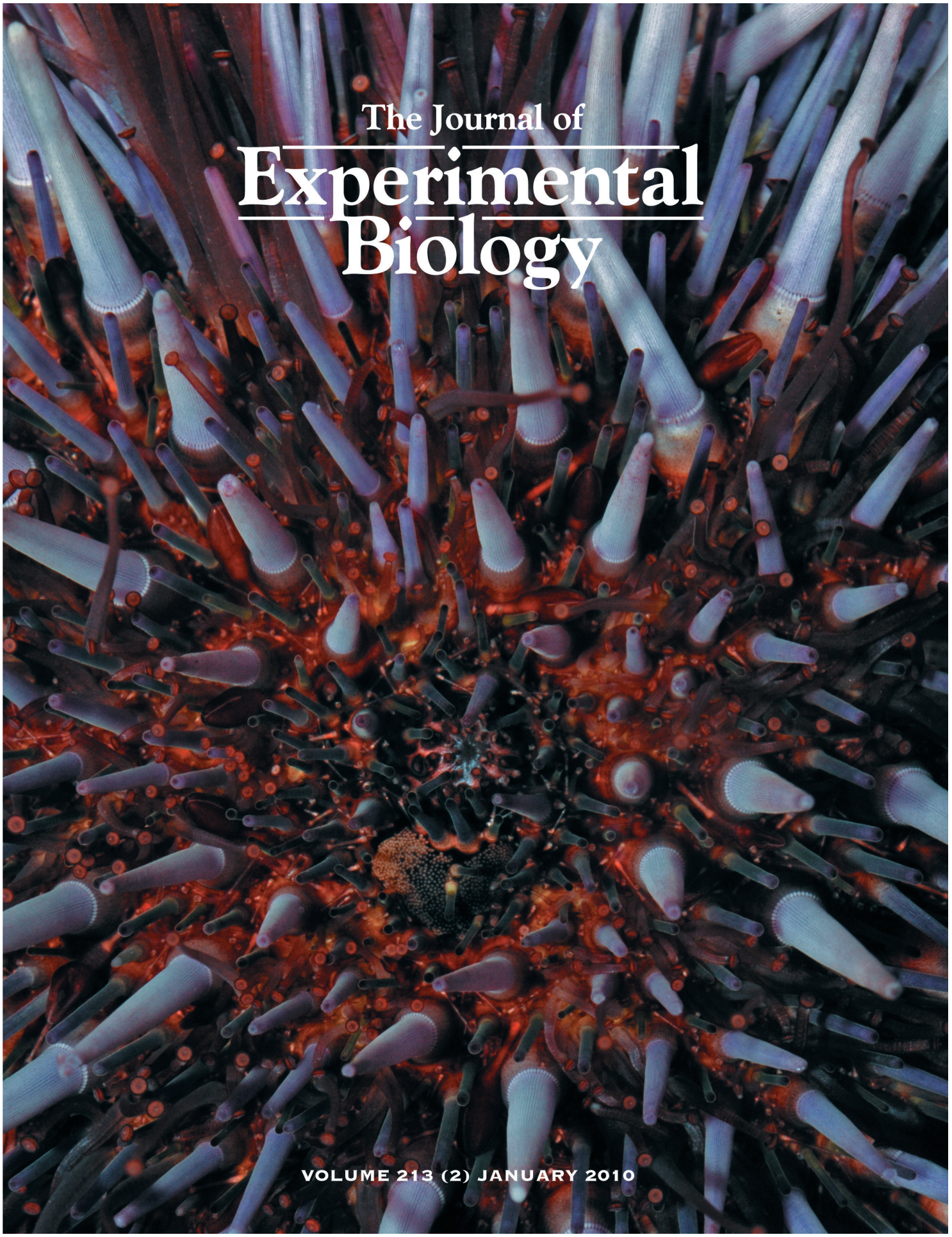
The Journal of
Experimental
Biology
VOLUME 213 (2) JANUARY 2010

The Journal of Experimental Biology 213, 249-255
Published by The Company of Biologists 2010
doi:10.1242/jeb.033159

Spatial vision in the purple sea urchin *Strongylocentrotus purpuratus* (Echinoidea)

D. Yerramilli and S. Johnsen*
Biology Department, Duke University, Durham, NC 27708, USA
*Author for correspondence (sjohnsen@duke.edu)

Accepted 14 October 2009

SUMMARY

Recent evidence that echinoids of the genus *Echinometra* have moderate visual acuity that appears to be mediated by their spines screening off-axis light suggests that the urchin *Strongylocentrotus purpuratus*, with its higher spine density, may have even more acute spatial vision. We analyzed the movements of 39 specimens of *S. purpuratus* after they were placed in the center of a featureless tank containing a round, black target that had an angular diameter of 6.5 deg. or 10 deg. (solid angles of 0.01 sr and 0.024 sr, respectively). An average orientation vector for each urchin was determined by testing the animal four times, with the target placed successively at bearings of 0 deg., 90 deg., 180 deg. and 270 deg. (relative to magnetic east). The urchins showed no significant unimodal or axial orientation relative to any non-target feature of the environment or relative to the changing position of the 6.5 deg. target. However, the urchins were strongly axially oriented relative to the changing position of the 10 deg. target (mean axis from –1 to 179 deg.; 95% confidence interval ± 12 deg.; $P<0.001$, Moore's non-parametric Hotelling's test), with 10 of the 20 urchins tested against that target choosing an average bearing within 10 deg. of either the target center or its opposite direction (two would be expected by chance). In addition, the average length of the 20 target-normalized bearings for the 10 deg. target (each the vector sum of the bearings for the four trials) were far higher than would be expected by chance ($P<10^{-10}$; Monte Carlo simulation), showing that each urchin, whether it moved towards or away from the target, did so with high consistency. These results strongly suggest that *S. purpuratus* detected the 10 deg. target, responding either by approaching it or fleeing it. Given that the urchins did not appear to respond to the 6.5 deg. target, it is likely that the 10 deg. target was close to the minimum detectable size for this species. Interestingly, measurements of the spine density of the regions of the test that faced horizontally predicted a similar visual resolution (8.3±0.5 deg. for the interambulacrum and 11±0.54 deg. for the ambulacrum). The function of this relatively low, but functional, acuity – on par with that of the chambered *Nautilus* and the horseshoe crab – is unclear but, given the bimodal response, is likely to be related to both shelter seeking and predator avoidance.

Key words: diffuse sensory system, echinoid, marine ecology, spatial vision, vision.

INTRODUCTION

Echinoderm photoreception is a well-studied but puzzling phenomenon. Light-mediated behaviors are ubiquitous in this phylum, including simple phototaxis, covering reactions, UV avoidance, homing, polarization sensitivity, color changes, shelter seeking, diurnal migrations and movement towards small dark objects (Millot, 1954; Millot, 1955; Thornton, 1956; Yoshida, 1966; Millot and Yoshida, 1960; Scheibling, 1980; Hendler, 1984; Johnsen, 1994; Johnsen and Kier, 1999; Adams, 2001; Blevins and Johnsen, 2004). However, the underlying architecture and abilities of this system have remained mysterious.

With the exception of the ocelli found at the tips of the arms of certain asteroids and the tentacular nerves of the holothurian *Opheodesoma spectabilis*, echinoderms have no discrete visual organs (reviewed by Yoshida et al., 1983). Instead, neurological and behavioral evidence suggests that their photosensitivity is diffuse and located above, below and even within the calcitic endoskeleton (Yoshida, 1979; Moore and Cobb, 1985; Aizenberg, 2001). More recently, Burke et al. (Burke et al., 2006) and Raible et al. (Raible et al., 2006) independently analyzed the genome of the echinoid *Strongylocentrotus purpuratus* and found six opsins from at least three pan-bilaterian families (r-opsin, c-opsin, G_o-opsin) that were most strongly expressed in the tube feet and the globiferous and tridentate pedicellariae (expression in the endoskeleton was not measured). While other recent work has found some remarkable adaptations in the endoskeleton of echinoderms, including polarizing filters, migrating pigments and arrays of microscopic lenses (Hendler, 1984; Johnsen, 1994; Aizenberg et al., 2001), no regional specialization akin to cephalization has been found, leaving open the question of the neurological and structural bases of these photobehaviors.

Woodley (Woodley, 1982) attempted to reconcile the ability of the tropical urchin *Diadema antillarum* to move towards small, dark objects with its apparent lack of an image-forming eye by suggesting that the entire animal functions as a compound eye, with the spines screening off-axis light, much like screening pigments optically separate ommatidia in insect eyes (Land and Nilsson, 2002). Blevins and Johnsen tested this hypothesis using echinoids of the genus *Echinometra* and found that their visual resolution was on the order of that predicted by the spacing of their spines (~30 deg.) (Blevins and Johnsen, 2004).

This paper examines the visual resolution of *S. purpuratus*. Like *Echinometra,* it exhibits shelter-seeking behavior and is known to have a photosensitive test. However, the angular density of its spines is roughly double–triple that of *Echinometra*. We therefore performed similar experiments to those described by Blevins and Johnsen (Blevins and Johnsen, 2004) to determine whether *S. purpuratus* had correspondingly higher visual resolution.

MATERIALS AND METHODS

Specimen collection and care

Twenty adult specimens of *Strongylocentrotus purpuratus* Stimpson 1857 were collected at Corona del Mar State Beach (33°35′N 117°52′W; Corona del Mar, CA, USA) by Charles Halloran, Inc. or obtained from Pat Leary at California Institute of Technology (Pasadena, CA, USA). They were kept in a covered aquarium at 15°C, under constant light, at a salinity of 30–35 p.p.t. While a 12 h:12 h light:dark cycle would have been preferable, captive *S. purpuratus* will often spawn in darkness, which fouls the water and can lead to significant mortality and morbidity. Because we found that even moderately unhealthy urchins did not move in the testing arena, they were kept under constant light and tested as soon as possible after collection (within two weeks).

Experimental apparatus

The experimental arena was similar to that used by Blevins and Johnsen (Blevins and Johnsen, 2004) and consisted of a covered fiberglass tank (1.2 m diameter) with a glass bottom (Fig. 1A). The covering of the tank had a small opening on one side and a large central circular opening that measured 0.4 m in diameter. A diffuse fluorescent light source was placed above the circular opening, resulting in a downwelling irradiance (integrated from 400–700 nm) at the arena floor of 4×10^{14} photons cm^{-2} s^{-1} [measured using an Ocean Optics USB2000 Spectroradiometer fitted with a CC3 cosine corrector, Dunedin, FL, USA; Fig. 1B). The tank was mounted on four cement blocks, and white cloth was placed directly under the glass bottom to allow unobtrusive observation of the urchins' shadows from below. The cloth was marked with a 32 cm diameter circle centered at the middle of the arena and divided into 15 deg. increments.

A black circular plastic target (5% diffuse reflectance, 1% specular reflectance) with a diameter of either 6 cm or 9 cm was attached to the wall of the tank. At this distance from the center of the arena (0.52 m), the diameters of the two targets subtended angles of ~6.5 deg. and 10 deg. (and their areas subtended solid angles of 0.01 sr and 0.024 sr). The reflectance of the arena wall was ~50% from 450–500 nm (the likely predominant wavelengths for echinoid photosensitivity), giving the target a Weber contrast of –0.9.

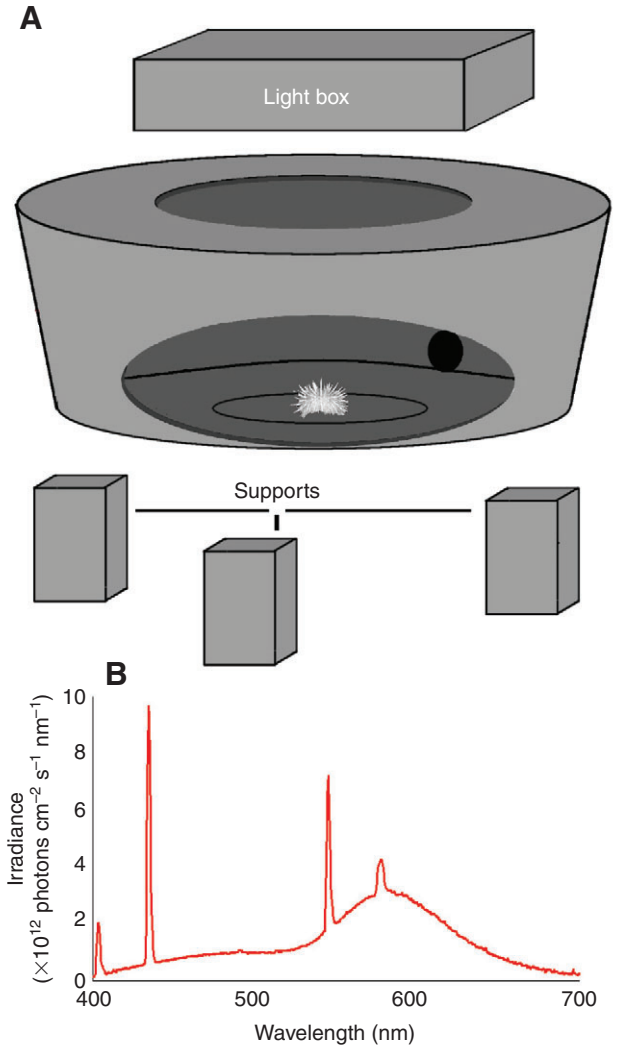

Fig. 1. (A) Diagram of testing arena. The circular black target can be seen on the back of the inside of the tank. The circle around the urchin denotes the distance the urchins must move before their bearing is recorded (16 cm). The elliptical hole in the side of the tank serves only to show the inside and is not found on the actual tank. (B) Downwelling spectral irradiance at the center of the arena.

Experimental procedure

On each day of trials, the arena was filled with artificial seawater of the same temperature and salinity as that in the holding aquarium. Each urchin was tested four times in a row, with the target placed successively at 0 deg., 90 deg., 180 deg. and 270 deg. (relative to magnetic east). The four different target positions allowed us to control for any spurious orientation to other features of the arena, room or external environment. The urchin was first placed in the center of the tank. Then the arena door was closed, the lights were turned on and the movement of the urchin was observed from below. The urchins generally began moving within 60 s, almost always in a straight line. Once the urchin moved 16 cm from the center, its bearing was recorded to the nearest 15 deg. Animals were stopped at 16 cm so that the angular size of the target (as viewed by the urchin) would not change significantly and potentially affect the results. The maximum angular diameters of the 6.5 deg. and 10 deg. targets at 16 cm from the center occurred when the animal moved directly towards the target and were 9.5 deg. and 14 deg., respectively. The minimum angular diameters of the targets at 16 cm from the center occurred when the animal moved directly away the target and were 5.0 deg. and 7.5 deg. Given that the animals moved in a straight line, the choice was almost certainly made based on the perception of angular size from the center of the arena. After the trial, the light was then turned off, the urchin was returned to a holding tank and the arena was scrubbed to reduce the potential for trail following. Then the urchin was returned to the center of the arena for the additional three trials (with randomly ordered target bearings). After the four trials, the mean absolute bearing ($\vec{\mathbf{V}}_{\mathrm{abs}}$) for a given urchin was calculated using:

$$\vec{\mathbf{V}}_{\mathrm{abs}} = \left(V_x, V_y\right) = \tfrac{1}{4}\left(\sum_{i=1}^{4}\cos\varphi_i, \sum_{i=1}^{4}\sin\varphi_i\right), \qquad (1)$$

where φ_i was the bearing of the urchin in the ith trial (relative to magnetic east) (Fig. 2A). The average bearing vector corrected ($\vec{\mathbf{V}}_{\mathrm{corrected}}$) for the moving position of the target (referred to hereafter as the target-normalized bearing) is:

$$\vec{\mathbf{V}}_{\mathrm{corrected}} = \left(V_x, V_y\right) = \tfrac{1}{4}\left(\sum_{i=1}^{4}\cos\left(\varphi_i - \omega_i\right), \sum_{i=1}^{4}\sin\left(\varphi_i - \omega_i\right)\right), \qquad (2)$$

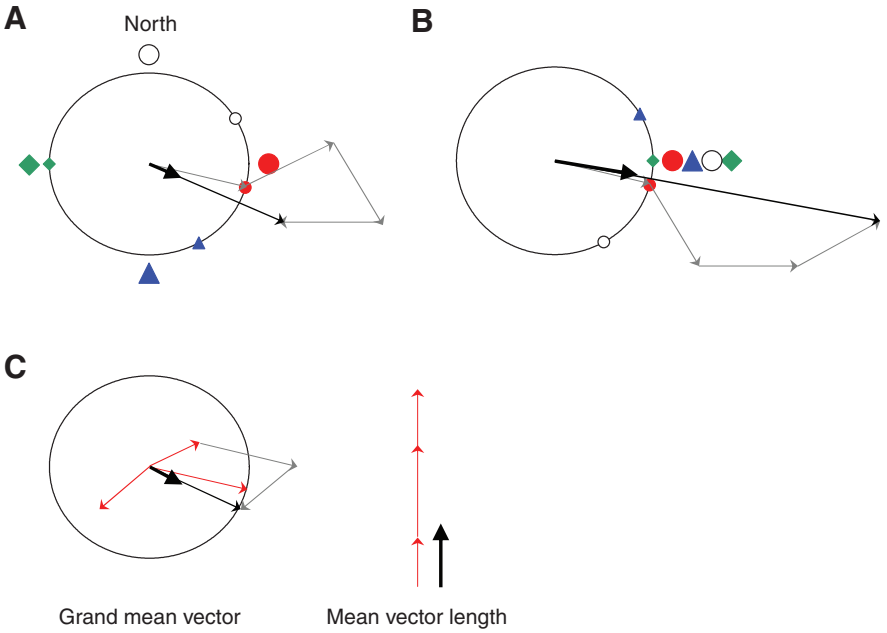

Fig. 2. Description of analysis. (A) Calculation of mean vector for the four absolute bearings of one urchin (symbols on circle) where the target is placed at the four compass points (matching larger symbols outside circle. The mean vector (bold short arrow) is one-quarter of the vector sum of the four bearing vectors (individual vectors in gray, sum vector in black, calculated using Eqn 1). (B) Calculation of the mean vector for target-normalized bearings (using Eqn 2). (C) Explanation of difference between the calculation of grand mean vector and that of average vector length for three sample urchins. The grand mean vector was calculated for both absolute and target-normalized vectors but in this example is done for target-normalized bearings. Each red arrow is the mean target-normalized vector (calculated using Eqn 2 based on four trials) for one urchin. The grand mean vector is one-third of the vector sum of the three mean vectors (calculated using Eqn 5). The average vector length is one-third of the simple sum of the lengths of the three mean vectors. The surrounding black circles in all three panels denote a vector length (*R*) of one.

where ω_i was the bearing of the target (0 deg., 90 deg., 180 deg. or 270 deg.) in the *i*th trial (Fig. 2B). As mentioned above, these corrected bearings control for orientation to other features in the environment. If the urchins are detecting the target and moving at some set angle relative to it, the corrected bearing vectors will remain consistent while the absolute bearings will be scattered.

For both the absolute and target-normalized bearings, the length of $\vec{\mathbf{V}}$ (generally referred to as '*R*' in circular statistics) is given by:

$$R = \left|\vec{\mathbf{V}}\right| = \sqrt{V_x^2 + V_y^2} \ . \tag{3}$$

In this case, *R* is a measure of the consistency of the headings of a given urchin over its four trials, with *R*=1 implying that the animal moved in the same direction (either absolute or relative to the target) all four times. Monte Carlo methods (see below) show that, for the four trials, the value of *R* expected by chance has a wide distribution centered around 0.45 (i.e. the average length of the vector sum of four randomly oriented unit vectors is 4×0.45=1.8).

The average angle over the four trials (θ) is given by:

$$\theta = \tan^{-1}\left(\frac{V_y}{V_x}\right)(+180 \text{ deg. if } V_x < 0) \ . \tag{4}$$

The grand mean vector ($\vec{\mathbf{V}}_{GM}$) for all of the 20 trials (which was used for testing for significant orientation of the urchins) was calculated for both absolute and target-normalized bearings using:

$$\vec{\mathbf{V}}_{GM} = \frac{1}{20}\left(\sum_{j=1}^{20}\cos\theta_j, \sum_{j=1}^{20}\sin\theta_j\right) , \tag{5}$$

where θ_j is the average bearing of the *j*th urchin calculated using Eqn 4. The length and angle of the grand mean vector are calculated using equations analogous to Eqns 3 and 4. It is important to note that the length of the grand mean vector is not the same as the average of the lengths of the vectors for each animal, because it is a vector sum and thus takes the directions of each vector into account. For example, if six urchins were tested and three always went directly towards the target (in all four trials) and three always went directly away from it, the length of the grand mean vector would be zero, but the average of the lengths of the vectors for the urchins would be 1, i.e. even though the group as a whole did not choose one direction relative to the target, they obviously responded to it. This is analogous to a group of people each using their own compass to go a different direction.

Data analysis

The collection of bivariate data (R_j,θ_j) was tested for significant orientation using either Hotelling's test or, if either of the *x* or *y* components of the bearings were not normally distributed, a non-parametric version of Hotelling's test developed by Moore (Moore, 1980) (but see Batschelet, 1981). Tests for significant unimodal and axial orientation were performed for both absolute bearings and target-normalized bearings.

Preliminary examination of the data suggested that the mean vectors for the target-normalized bearings for the 10 deg. target (calculated using Eqn 3) were unusually long. This was tested in two ways. First, cumulative histograms of the mean vector lengths of absolute and target-normalized bearings were compared with that expected due to random chance using the Kolmogorov–Smirnov test. In addition, because it is extremely difficult to accurately determine the Kolmogorov–Smirnov distribution for very low *P*-values, Monte Carlo methods were also used to test whether the average length of the 20 mean vectors was non-random. Ten billion (10^{10}) runs of 20 urchins, each run four times with random bearings, were generated. The average of the mean vector lengths was calculated for each run (note that this is NOT the length of the grand average vector):

$$\bar{R} = \frac{1}{20}\sum_{i=1}^{20} R_i \ . \tag{6}$$

A histogram of 10^{10} $\bar{R}$'s was generated and compared with the experimental value. The Monte Carlo simulation was programmed using Matlab (Mathworks, Natick, MA, USA).

RESULTS

Bearings of urchins using 6.5 deg. target

The absolute bearings, uncorrected for the position of the target, showed no significant unimodal or axial orientation (Fig. 3A, Table 1). The target-normalized bearings also showed no significant

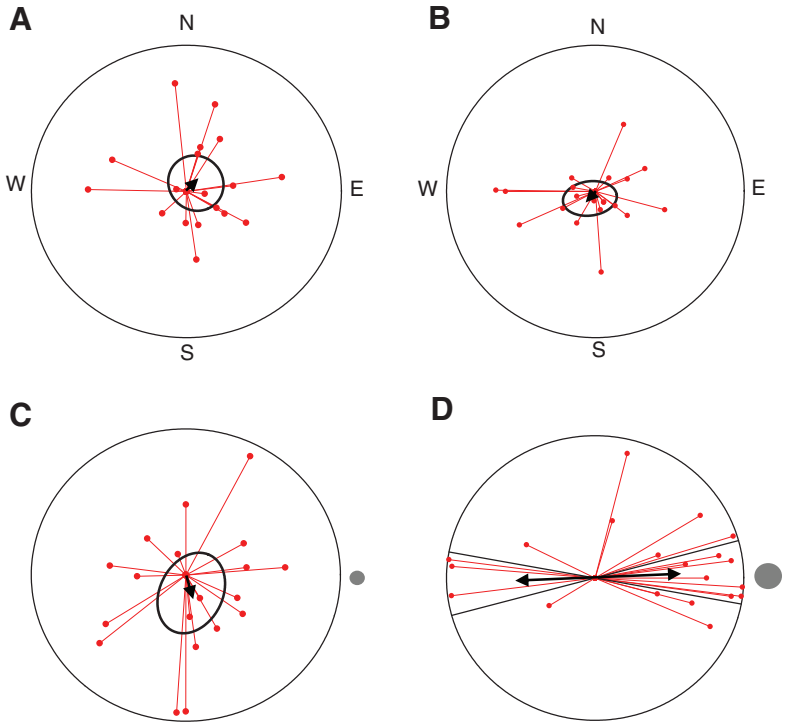

Fig. 3. (A) The absolute average bearings for each echinoid tested against the 6.5 deg. target (averaged over their four trials) (N, E, W and S are geomagnetic compass points). (B) The absolute average bearings for each echinoid tested against the 10 deg. target. (C) The average bearings relative to the position of the 6.5 deg. target (shown to scale in gray at the right of the graph). (D) The average bearings relative to the position of the 10 deg. target (shown to scale in gray at the right of the graph). The red lines show the length and direction of the average bearing for the four trials with one echinoid. Red lines that reach the outer circle imply that the echinoid went the same direction in all four trials (either un-normalized or relative to the target). The bold black lines show the average vector sum of the 20 average bearings, also known as the grand mean vector. Only the grand mean vector for unimodal orientation is shown in A, B and C, and only the grand mean vector for axial orientation is shown in D. The black ellipses in A–C are 95% confidence ellipses for the magnitude and direction of the grand mean vector (i.e. the endpoint of the bold, black arrow has a 95% confidence of lying within the ellipse. The boundaries of the 95% confidence interval for the mean angle of the grand mean vector are also shown in black in D (a confidence ellipse cannot be used because the data is not normal). The large surrounding black circles in all four panels denote a vector length (R) of one.

unimodal or axial orientation (Fig. 3C; Table 1). The distribution of the lengths of the absolute vectors relative to that expected by chance was borderline significant (P=0.044, Kolmogorov–Smirnov test). The distribution of the lengths of the target-normalized vectors was not significantly different from chance (Table 1).

Bearings of urchins using 10 deg. target

The absolute bearings showed no significant unimodal or axial orientation (Fig. 3B, Table 1). Analyzed unimodally, the target-normalized bearings also showed no significant orientation. However, the target-normalized bearings were axially oriented with high significance (mean axis from –1 to 179 deg.; 95% confidence interval±12 deg.; P<0.00025), with 10 out of the 20 urchins choosing an average bearing within 10 deg. of either the target or its opposite direction (Fig. 3D, Table 1). The distribution of the lengths of the target-normalized vectors was significantly different from chance (P≪0.001, Kolmogorov–Smirnov test), with an average vector length of 0.77±0.05 – far higher than the expected average of 0.45 (P<10^{-10}, Monte Carlo simulation). The distribution of the lengths of the absolute vectors was also significantly different from that expected by chance (P<0.001, Kolmogorov–Smirnov Test), with an average vector length of 0.29±0.04 – lower than the expected average of 0.45 (P<0.001, Monte Carlo simulation). It is important to note that, because the target is moved to four different positions, an urchin that follows it will have a long target-normalized bearing vector and a short absolute bearing vector.

Table 1. Absolute and target-normalized bearings of urchins

Bearings	θ (grand mean, deg.)	95% confidence	R (grand mean)	P-value (orientation)	R (average length)	P-value (R lengths)
6.5 deg. target (N=19)						
Absolute						
Unimodal	–118	–	0.083	n.s.*	0.36	0.044‡
Axial	175–355	–	0.016	n.s.*	–	–
Target-normalized						
Unimodal	74	–	0.13	n.s.*	0.51	n.s.‡
Axial	110–290	–	0.090	n.s.*	–	–
10 deg. target (N=20)						
Absolute						
Unimodal	–140	–	0.060	n.s.*	0.29	<0.001‡
Axial	80–260	–	0.096	n.s.*	–	–
Target-normalized						
Unimodal	–15	–	0.34	n.s.†	0.77	<10^{-10}§
Axial	–2.3–178	±13 deg.	0.55	<0.001†	–	–

*Hotelling's one-sample test.
†Moore's non-parametric test for bivariate data.
‡Kolmogorov–Smirnov test.
§Monte Carlo simulation.

DISCUSSION

Two aspects of the results strongly suggest that *S. purpuratus* was able to detect a 10 deg. diameter target whose solid angle was less than 0.2% of the total visual field. First, as a population, the animals were strongly axially oriented, with half of them orienting to within 10 deg. of the target center or its opposite bearing. Second, the orientation of individual animals was remarkably strong, with almost all of the urchins moving consistently either towards or away from the target as it was placed at four different bearings.

The bimodal nature of the response (and its consistency over four trials for a given animal) suggests that it is unlikely to be a simple phototaxis. Also, measurements using the spectroradiometer described above showed that the horizontal irradiance on the side of the urchin facing the dark target is only 1% less than that on the side of the urchin facing away from the target – less than the ~5% azimuthal variation of horizontal irradiances in an empty arena measured over the eight compass points. Therefore, any response based on only the irradiance at the surface of the urchin would have been even more strongly affected by the slight (but larger) azimuthal variation in the arena irradiance and lead to significant orientation of the absolute bearings. Also, the variations in horizontal irradiance in even the most uniform underwater environment are far higher than 1–5% and also vary continually, suggesting that movements based on irradiance changes of a few percent would be maladaptive.

With the exception of one borderline significant result (that either Bonferroni correction or control of false discovery rate eliminates) there was no evidence that the urchins responded to the 6.5 deg. target, suggesting that the 10 deg. target is close to the lower threshold of what can be detected by *S. purpuratus*. However, it is important to note that the exact spatial resolution of *S. purpuratus* cannot be determined from the results of this study because a single object on an empty background can be detected by visual systems with lower resolution than the object's size. However, calculations by Blevins and Johnsen (Blevins and Johnsen, 2004) showed that objects significantly smaller than the resolution limit of a viewer can only be detected if the viewer is sensitive to very small changes in brightness over graded boundaries (luminous objects on a black background such as stars are an exception because their contrast is essentially infinite). Some aquatic vertebrates can detect radiance differences of ~1–2% under ideal conditions (Douglas and Hawryshyn, 1990). However, the regions with the differing radiances must be adjacent and separated by a sharp border (Land and Nilsson, 2002). Gradual changes in radiance are far more difficult to detect. Thus, the spatial resolution of *S. purpuratus* is likely to be at least 10 deg. It is, of course, possible that the urchins possess higher acuity but were not motivated to move towards or away from the smaller target (perhaps not perceiving it as large enough to be a threat or useful shelter). This classical issue of motivation *versus* perception is difficult to address in any experimental system. At present though, there is no proposed optical mechanism for higher acuity.

This resolution is consistent with the hypothesis that spatial vision in echinoids is mediated by screening of off-axis light by the spines, much like photostable pigments screen off-axis light in compound eyes. In the regions of the test of *S. purpuratus* that faced horizontally, spines were spaced by about 4 deg. in the interambulacrum and 5.5 deg. in the ambulacrum (Fig. 4, see caption for details of measurements). Given that the test is convex and that the spines are more or less perpendicularly to its surface, on average

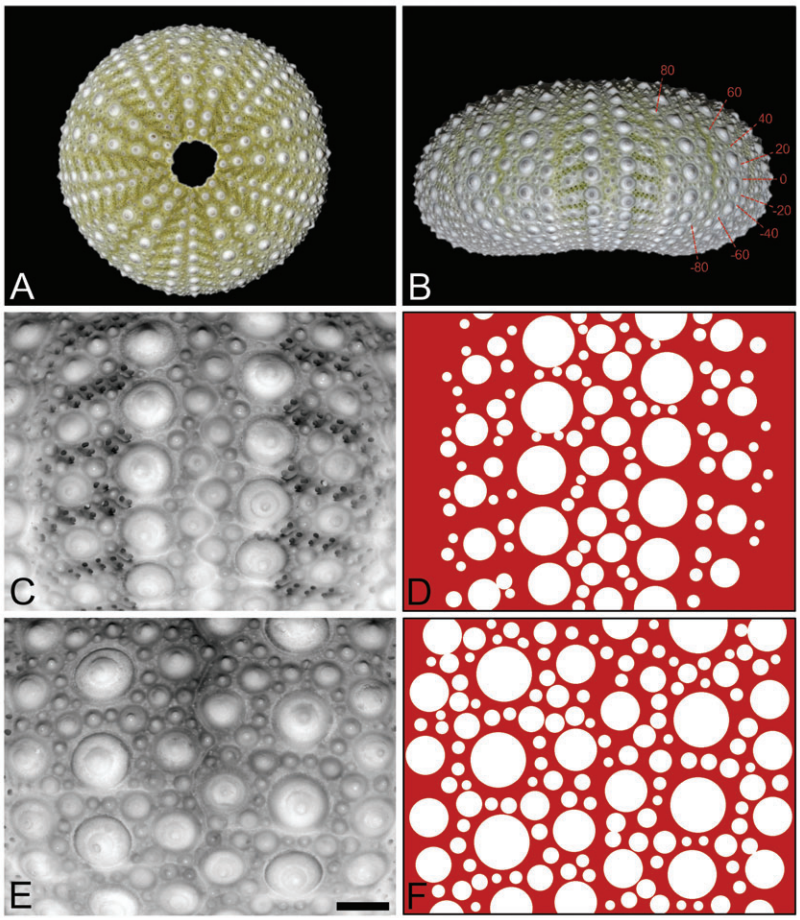

Fig. 4. Denuded test of *Strongylocentrotus purpuratus* showing spine density. (A) Plan view. (B) Profile view showing angles of vectors normal to the surface. (C) Portion of ambulacrum (region with tube feet). (D) Diagram of ambulacrum region shown in C. (E) Portion of interambulacrum. (F) Diagram of interambulacrum region shown in E. Regions shown in C and E are those that face horizontally, because those are the most likely to be involved in detecting targets on the horizon. Red portions of D and F indicate regions of the test that are not covered by the base of a spine and thus most likely to be photosensitive. Scale bar is 5 deg. in the horizontal direction and 15 deg. in the vertical direction (the vertical curvature is higher than the horizontal curvature in this region of the test). The horizontal spine densities quoted in the text were calculated by drawing 17 evenly spaced horizontal lines across both the ambulacrum and interambulacrum and counting the number of intersections with spines.

any given photosensitive region of the horizontally facing portion of the test and pedicellariae would have its horizontal field of view restricted to about 4–5.5 deg. [see Blevins and Johnsen for figures and further details (Blevins and Johnsen, 2004)]. From signal theory, detail can be resolved over angles that are double the angular resolution of the detector (Land and Nilsson, 2002), so, based on spine density, *S. purpuratus* is predicted to have a spatial resolution of 8–11 deg., which approximates the experimental results. The urchins *Echinometra lucunter* and *Echinometra viridis* moved towards 33 deg. targets but not towards 26 deg. or 16 deg. targets (Blevins and Johnsen, 2004). Similar measurements on this genus show that the horizontal density of the spines in the horizontal-facing region of their test is about 12.5 deg. (interambulacrum) and 9.5 deg. (ambulacrum), predicting a horizontal acuity between 19 deg. and 25 deg. in the horizontal direction [slightly higher than the global spine density given in Blevins and Johnsen (Blevins and Johnsen, 2004), due to regional variation]. This is somewhat better than the behavioral results show, suggesting that other factors, ranging from motivation to other morphological features of the test and pedicellariae, also play a role. Another issue is that the spacing of the spines is highly variable, depending on the exact region of the test, so exact predictions are problematic. Unfortunately, because clipping or removing substantial numbers of spines drastically affects both the locomotion and the health (and thus motivation) of the urchins, a more direct test of the hypothesis that the spine density mediates spatial vision is not possible. However, morphological studies of the tests and pedicellariae of echinoids have found no evidence for the screening of off-axis light (reviewed by Yoshida et al., 1983), leaving the spines as the most likely candidate to mediate this level of visual acuity.

The ecological function of movement towards and away from small dark objects in *S. purpuratus* is unknown, but is likely to be related to shelter seeking and predator avoidance, respectively. *Strongylocentrotus purpuratus*, found on the west coast of North America, mostly resides in shallow, wave-swept habitats, foraging on drifting algal detritus or grazing on attached plants (Workman, 1999; Tegner, 2001). When these food items become scarce, the urchins switch to active foraging (Tegner, 2001), which would presumably be enhanced by even moderate visual acuity. Additionally, *S. purpuratus*, like *Echinometra*, is often found in small, dark boreholes – presumably to protect them from wave forces and predation – that they would need to locate after foraging (Verling et al., 2004). While intertidal populations move very little, and can actually become trapped for life in their boreholes, subtidal populations (from which the experimental animals were drawn) may migrate over moderate distances for spawning or foraging (reviewed by Workman, 1999). Spatial vision may also facilitate the aggregation that can precede mass spawning. Finally, while visual detection offers no real protection against their primary predator, sea otters, it may allow *S. purpuratus* to successfully retreat from its slower predators, such as the sea stars *Pycnopodia helianthoides* and *Pisaster ochraceus*.

We originally expected that the urchins would move consistently towards the target, based on the shade-seeking behavior found in certain other echinoderms (e.g. Johnsen and Kier, 1999; Aizenberg et al., 2001; Adams, 2001). In particular, the congeneric species *Strongylocentrotus droebachiensis* seeks shade, although only in the presence of UV radiation (Adams, 2001). However, one quarter of the specimens of S. *purpuratus* moved consistently and directly away from the target. We speculate that the two behaviors represent two different motivational states related to opposing interpretations of the target, mostly likely to be shelter *versus* predator. Distinguishing a predator from a harmless or beneficial target (e.g. shelter, conspecific) is a difficult problem for species with low-resolution vision and is likely to be particularly problematic for urchins given their low visual acuity and slow movements. Some species solve this problem using simple rules. For example, the fiddler crab *Uca pugilator*, which has a resolution of 1–5 deg., sorts predators from conspecifics entirely by their position relative to the horizon, with anything above the horizon being considered a (presumably avian) predator (Land and Layne, 1995; Zeil and Hemmi, 2005). The snapping shrimp *Synalpheus demani* apparently sorts shade from predator by angular size, approaching 90 deg. or larger targets and fleeing from 30 deg. targets (Huang et al., 2005). The ophiuroid *Ophiocoma wendtii* responds in a similar manner, fleeing from shadows cast on it and moving towards dark regions on the horizon (Aizenberg et al., 2001). Future studies will examine whether the target's position, shape or size affects the polarity of the urchins' responses.

Finally, it is possible that the polarity of the response is cyclical, as was found in the amphipod *Talitrus saltator*, which moves alternately towards or away from small dark object depending on time of day, with a pattern that matched its natural migrations up and down the beach (Scapini, 1997). While the tests in the present study were all performed within a relatively narrow time window during the middle of the day, it is nevertheless possible that individuals were at different points in some endogenous rhythm that affected behavior.

In conclusion, the spatial visual resolution in *S. purpuratus* appears to be predicted by the density of its spines, lending further support to the hypothesis that at least some echinoids operate as large compound eyes. The resolution of the system is far lower than that of vertebrate camera eyes but roughly equal to that of the chambered *Nautilus* and the horseshoe crabs, suggesting that the visual behavior of echinoids may be more complex than previously appreciated.

ACKNOWLEDGEMENTS

We thank Drs David McClay and Gregory Wray for the use of their urchins and Drs Alison Sweeney, Eric Warrant and Tamara Frank for comments on earlier drafts. S.J. was supported in part by a grant from the National Science Foundation (IOB-0444674).

REFERENCES

Adams, N. (2001). UV radiation evokes negative phototaxis and covering behavior in the sea urchin *Strongylocentrotus droebachiensis*. *Mar. Ecol. Prog. Ser.* **213**, 87-95.
Aizenberg, J., Tkachenko, A., Weiner, S., Addadi, L. and Hendler, G. (2001). Calcitic microlenses as part of the photoreceptor system in brittlestars. *Nature* **412**, 819-822.
Batschelet, E. (1981). *Circular Statistics in Biology*. New York: Academic Press.
Blevins, E. and Johnsen, S. (2004). Spatial vision in the echinoid genus *Echinometra*. *J. Exp. Biol.* **207**, 4249-4253.
Burke, R. D., Angerer, L. M., Elphick, M. R., Humphrey, G. W., Yaguchi, S., Kiyama, T., Liang, S., Mu, X., Agca, C., Klein, W. H. et al (2006). A genomic view of the sea urchin nervous system. *Dev. Biol.* **300**, 434-460.
Hendler, G. (1984). Brittlestar color change and phototaxis (Ophiocomidae). *PSZNI Mar. Ecol.* **5**, 9-27.
Huang, H.-D., Rittschoff, D. and Jeng, M.-S. (2005). Visual orientation of the symbiotic snapping shrimp *Synalpheus demani*. *J. Exp. Mar. Biol. Ecol.* **326**, 56-66.
Johnsen, S. (1994). Extraocular sensitivity to polarized light in an echinoderm. *J. Exp. Biol.* **195**, 281-291.
Johnsen, S. and Kier, W. M. (1999). Shade-seeking behavior under polarized light by the brittlestar *Ophioderma brevispinum*. *J. Mar. Biol. Assoc. UK* **79**, 761-763.
Land, M. F. and Layne, J. (1995). The visual control of behaviour in fiddler crabs: I. Resolution, thresholds and the role of the horizon. *J. Comp. Physiol. A* **177**, 81-90.
Land, M. F. and Nilsson, D.-E. (2002). *Animal Eyes*. Oxford University Press, New York.
Millot, N. (1954). Sensitivity to light and the reactions to changes in light intensity of the echinoid *Diadema antillarum Philippi*. *Phil. Trans. Roy. Soc. B.* **238**, 187-220.
Millot, N. (1955). The covering reaction in a tropical sea urchin. *Nature* **175**, 561.
Millot, N. and Yoshida, M. (1960). The shadow reaction of *Diadema antillarum*: the spine response and its relation to the stimulus. *J. Exp. Biol.* **37**, 363-375.
Moore, A. and Cobb, J. L. S. (1985). Neurophysiological studies on photic responses in *Ophiura ophiura*. *Comp. Biochem. Physiol.* **80A**, 11-16.
Moore, B. R. (1980). A modification of the Rayleigh test for vector data. *Biometrika* **67**, 175-180.

Raible, F., Tessmar-Raible, K., Arboleda, E., Kaller, T., Bork, P., Arendt, D. and Arnone, M. (2006). Opsins and clusters of sensory G-protein coupled receptors in the sea urchin genome. *Dev. Biol.* **300**, 461-475.

Scapini, F. (1997). Variation in scototaxis and orientation adaptation of *Talitrus saltator* populations subjected to different ecological constraints. *Estuar. Coast. Shelf Sci.* **44**, 139-146.

Scheibling, R. E. (1980). Homing movements of *Oreaster reticulatus* when experimentally translocated from a sand patch habitat. *Mar. Behav. Physiol.* **7**, 213-223.

Tegner, M. J. (2001). The ecology of *Strongylocentrotus franciscanus* and *Strongylocentrotus purpuratus*. *Edible Sea Urchins: Biology and Ecology*. New York: Elsevier.

Thornton, I. W. B. (1956). Diurnal migrations of the echinoid *Diadema setosum*. *Brit. J. Anim. Behav.* **4**, 143-146.

Verling, E., Crook, A. C. and Barnes, D. K. A. (2004). The dynamics of covering behaviour in dominant echinoid populations from American and European west coasts. *Mar. Ecol.* **25**, 191-206.

Woodley, J. D. (1982). Photosensitivity in *Diadema antillarum*: does it show scototaxis? In *The International Echinoderm Conference, Tampa Bay* (ed. J. M. Lawrence), pp. 61. Rotterdam: A. A. Balkema.

Workman G. (1999). *A Review of the Biology and Fisheries for Purple Sea Urchin* (*Strongylocentrotus purpuratus*, *Stimpson, 1957*) *and Discussion of the Assessment Needs of a Proposed Fishery*. Canadian stock assessment secretariat research document 99/163. Fisheries and Oceans Canada, Ottawa.

Yoshida, M. (1966). Photosensitivity. In *Physiology of Echinodermata* (ed. R. A. Boolootian), pp. 435-464. New York: John Wiley and Sons.

Yoshida, M. (1979). Extraocular photoreception. In *Handbook of Sensory Physiology* vol. 7/6A (ed. H. Autrum), pp. 581-640. New York: Springer-Verlag.

Yoshida, M., Takasu, N. and Tamotsu, S. (1983). Photoreception in echinoderms. In *Photoreception and Vision in Invertebrates* (ed. M. A. Ali), pp. 743-772. New York: Plenum Press.

Zeil, J. and Hemmi, J. M. (2005). The visual ecology of fiddler crabs. *J. Comp. Physiol. A* **192**, 1-25.

Inside JEB highlights the key developments in *The Journal of Experimental Biology*. Written by science journalists, the short reports give the inside view of the science in JEB.

Inside JEB

BEES USE THREE-PHASE LANDING STRATEGY

Mandyam Srinivasan is an electrical engineer that is intrigued by bees. 'I have been fascinated for a long time how a creature with a brain the size of a sesame seed can do all of the things that it does,' says Srinivasan. Over the course of his career, Srinivasan has discovered how insects negotiate the world by analysing how images of the surroundings move across the eye rather than using stereovision. Having discovered how bees use this 'optic flow' information to negotiate the environment, regulate their flight speed and control their approach during landing, Srinivasan began wondering what happens in the final moments of a touchdown. Flies landing on a ceiling simply grab hold with their front legs and somersault up as they zip along, but Srinivasan knew that a bee's approach is more sedate. Curious to know more about bee landing techniques, Srinivasan teamed up with Carla Evangelista, Peter Kraft, Marie Dacke and Judith Reinhard and used a high-speed camera to film the instant of touch-down on surfaces at various inclinations (p. 262).

First, the team built a bee-landing platform that could be inclined at any angle from horizontal to inverted (like a ceiling); they then trained bees to land on it and began filming. Having collected movies of the bees landing on surfaces ranging from 0 deg. to 180 deg., and every 10 deg. inclination between, Evangelista began the painstaking task of manually analysing the bees' landing tactics and saw that the bees' approach could be broken down into three phases.

Initially, the bees approached from almost any direction and at any speed; however, as they got closer to the platforms, they slowed dramatically, almost hovering, until they were 16 mm from the platform, when they ground to a complete halt, hovering for anything ranging from 50 ms to over 140 ms. When the surface was horizontal or inclined slightly, the bees' hind legs were almost within touching distance of the surface, so it was simply a matter of the bee gently lowering itself and grabbing hold with its rear feet.

However, when the insects were landing on surfaces ranging from vertical to inverted 'ceilings', their antennae were closest to the surface during the hover phase. When the antennae grazed the surface, this triggered the bees to reach up with the front legs, grasp hold of the surface and then slowly heave their middle and hind legs up too. 'We had not expected the antennae to play a role, and the fact that there is a mechanical aspect of this is something that we hadn't thought about,' admits Srinivasan.

Looking at the antennae's positions, the team realised that the bees held them roughly perpendicular to the surface in the final stages when approaching inverted surfaces. 'The bee is able to estimate the slope of the surface to orient correctly the antennae, so it is using its visual system,' explains Srinivasan. But this is surprising, because the insects are almost completely stationary while hovering and unable to use image movement across the eye to estimate distances. Srinivasan suspects that the bees could be using stereovision over such a short distance and is keen to test the idea.

Finally the team realised that bees are almost tailor-made to land on surfaces inclined at angles of 60 deg. to the horizontal. 'When bees are flying fast their bodies are horizontal, but when they are flying slowly or hovering their abdomen tilts down so that the tips of the legs and antennae lie in a plane that makes an angle of 60 deg.' explains Srinivasan: so the legs and antennae all touch down simultaneously on surfaces inclined at that angle. 'It seems like they are adapted to land on surfaces tilted to 60 deg. and we are keen to find out whether many flowers have this natural tilt,' says Srinivasan.

10.1242/jeb.041483

Evangelista, C., Kraft, P., Dacke, M., Reinhard, J. and Srinivasan, M. V. (2010). The moment before touchdown: landing manoeuvres of the honeybee *Apis mellifera*. *J. Exp. Biol.* **213**, 262-270.

SEA URCHINS USE WHOLE BODY AS EYE

Sea urchins don't seem to have any problems avoiding predators or finding comfortable dark corners to hide in, but they appear to do all this without eyes. So how do they see? It appears that sea urchins may use the whole surface of their bodies as a compound eye, and the animals' spines may shield their bodies from light coming from wide angles to enable them to pick out relatively fine visual detail. Divya

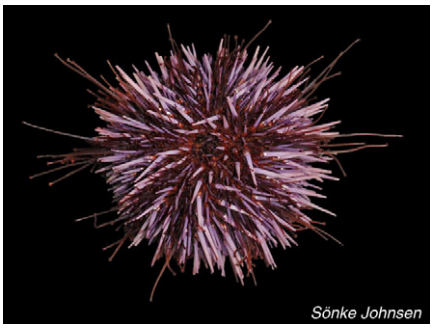

Yerramilli and Sönke Johnsen from Duke University explain that if this is the case, sea urchins with densely packed spines will have better vision than sea urchins with sparsely packed spines, so they decided to test the vision of *Strongylocentrotus purpuratus* sea urchins, with tightly packed spines, to find out how well they see (p. 249).

Placing individual urchins in a brightly lit arena with a 6 cm or 9 cm diameter dark disk on the arena's wall, the team viewed the shadows of the moving animals from beneath the arena's white floor. Would the sea urchins see the disk and respond to it, or would they be oblivious to the disk's presence? Recording 39 urchins' responses to the disk at different positions around the arena's perimeter, the duo saw that the urchins wandered randomly around the arena when the 6 cm diameter disk was in place; they didn't respond to it. But it was a different matter with the 9 cm diameter disk; the urchins either raced toward it or fled in the opposite direction.

Calculating the visual angle of the 9 cm diameter disk from a sea urchin's perspective, Yerramilli and Johnsen suggest that the sea urchin's visual resolution is at least 10 deg. And when the pair calculated the sea urchin's visual resolution based on the animal's spine density, they found that it could be as good as 8 deg., but not good enough to see the smaller 6 cm diameter disk.

But why did some of the sea urchins career toward the disk while others turned away? Yerramilli and Johnsen suspect that it depends on the sea urchin's interpretation of the dark object. Some of the animals may interpret the object as a predator and flee, while others identify it as shelter and head towards it. What is more surprising is that the urchins' vision is as good as *Nautilus* and horseshoe crab vision, which is quite impressive for an echinoid that has turned its whole body into an eye.

10.1242/jeb.041715

Yerramilli, D. and Johnsen, S. (2010). Spatial vision in the purple sea urchin *Strongylocentrotus purpuratus* (Echinoidea). *J. Exp. Biol.* **213**, 249-255.

TIMEFRAME AFFECTS SNAKES' ABILITY TO COPE WITH CLIMATE CHANGE

We're all at risk from climate change, but cold-blooded animals (ectotherms) that depend on the environment to maintain their body temperatures could be at more risk than most. And with weather patterns becoming more unstable, it may not just be a case of adapting to a warmer or cooler climate, but to more hot and cold snaps too. Curious to find out how ectotherms adapt to short- and long-term temperature changes, Fabien Aubret from the CNRS à Moulis, France, and Richard Shine from the University of Sydney, Australia, decided to find out how hatchling tiger snakes respond to cool and warm conditions (p. 242).

The duo built three habitats, each with an incandescent light bulb at one end to create a temperature gradient in the enclosure, and allowed the snakes to thermoregulate by basking where ever they found the temperature comfortable. The light bulb in one enclosure switched off when the ground temperature reached 22°C to create a cool environment, the bulb in the second enclosure switched off when the top temperature reached 26°C (warm environment), and the bulb in the third enclosure was on continually between 06.00 h and 21.00 h to make it really hot.

Monitoring the young snakes' health, growth and body temperatures over 14 months, the duo was surprised to see that, despite the snakes' dramatically different environments the young animals' ability to maintain similar mean and maximum body temperatures was impressive. The snakes had adapted their behaviour to ensure that they all maintained a similar body temperature, and the snakes in the cold enclosure had compensated for the cooler climate by basking for longer. However, the cold-adapted snakes seemed to have paid a price for survival in the cold: they were smaller than their warm-adapted siblings.

Aubret and Shine put the differences in the snakes' sizes down to several possibilities. They suggest that the cold snakes may be smaller because they have to devote more energy to finding warm basking spots, or it may simply be easier for small snakes to get warm compared with larger snakes. Alternatively, the warmer snakes could have grown larger because digestion is more efficient in warm conditions, allowing them to make the most of mice dinners.

So, young tiger snakes seem to be able to adapt to long-term environmental change, but how would they manage during a warm or cold snap? Could they adjust their behaviour to take account of a sudden change in temperature?

Aubret and Shine switched on all of the bulbs over the enclosures to warm all three climates as much as possible and watched how the snakes responded. Would they adjust their basking habits? They did not. The snakes that had grown up in cold conditions basked for longer than snakes that were used to the heat; and their body temepratures were warmer by 2.1°C. And when the team took away the lamps and plunged the snakes into a cold snap, the hot-adapted snakes' temperatures fell on average by 1.5°C because they basked for a fraction of the time that the cold-adapted snakes basked.

Despite adapting well to long-term climate conditions when they were young, the snakes were unable to adapt to short-term climate fluctuations when they were older. 'Our data provide a striking example of how an ectotherm's thermoregulatory tactics and mean selected body temperature can depend more upon previously encountered conditions than upon current thermal challenge,' say Aubret and Shine.

10.1242/jeb.041467

Aubret, F. and Shine, R. (2010). Thermal plasticity in young snakes: how will climate change affect the thermoregulatory tactics of ectotherms? *J. Exp. Biol.* **213**, 242-248.